

# DISTRIBUTED KALMAN FILTER-BASED TARGET TRACKING IN WIRELESS SENSOR NETWORKS

Phuong Pham and Sesh Commuri

*School of Electrical and Computer Engineering, The University of Oklahoma  
110 W. Boyd St., Devon Energy Hall 150, Norman, Oklahoma 73019-1102, U.S.A.*

**Keywords:** Distributed Kalman Filter, Wireless Sensor Networks, and Target Tracking.

**Abstract:** The tracking of mobile targets using Distributed Kalman Filters in a Wireless Sensor Network (WSN) is addressed in this paper. In contrast to the Kalman Filter implementations reported in the literature, our approach has the Kalman Filter running on only one network node at any given time. The knowledge learned by this node, i.e. the system state and the covariance matrix, is passed on to the subsequent node running the filter. Since a finite subset of the sensor nodes is active at any given time, target tracking can be accomplished using lower power compared to centralized implementations of the Kalman Filter. Numerical simulations demonstrate that the proposed algorithm is robust to measurement noise and changes in the velocity of the target. The results in this paper show that the proposed technique for target tracking will result in significant savings in power consumption and will extend the useful life of the WSN.

## 1 INTRODUCTION

Surveillance of remote inaccessible areas and the detection and tracking of intruders are some of the important applications of Wireless Sensor Networks (WSNs). Research in WSNs has addressed several important issues in optimal deployment, coverage, routing, and energy efficiency of the WSNs (Akyildiz, Su, Sankarasubramaniam, and Cayirci, 2002; Al-Karaki and Kamal, 2004; Cardei, Thai, Li, and Wu, 2005; Chiang, Wu, Liu, and Gerla, 1997; Watfa and Commuri, 2006a, 2006b). Diffusion and directed diffusion approaches have been proposed to address coverage, routing, discovering, and sensing fusion issues in WSNs (Intanagonwiwat, Govindan, and Estrin, 2000). The application of WSNs in surveillance and monitoring of target areas have also been widely researched (Chen, Gonzalez, and Leung, 2007). While the results presented in these papers are encouraging, their applicability in low cost WSNs with large measurement noise and faulty measurements is fraught with problems. In recent years, Kalman Filters have been proposed to address the uncertainty and the noise in the measurements (Rao and Durrant-Whyte, 1991; Olfati-Saber, 2007; Alriksson and Rantzer, 2007; Olfati-Saber and Shamma, 2005; Cattivelli, Lopes, and Sayed, 2008;

Uhlmann, 1996; Kim, West, Scholte, and Narayanan, 2008; Mutambara, 1998; Hashemipour, Roy, and Laub, 1998). Both centralized and distributed implementation of the Kalman Filter was proposed to make their use suitable to WSN applications. However, these techniques are still power intensive and require significant amounts of onboard power for communication and computation.

Two classes of Kalman filtering approaches have been implemented in WSNs. The first approach is centralized Kalman Filters (Rao, et al., 1991) where every sensor node takes measurements and communicates with the other nodes while simultaneously performing its own version of Kalman Filter. In this approach, the sensor nodes' power will be depleted quickly because of excessive measurements and inter-node communication. Moreover, it is sometimes impractical for a sensor node to communicate with all the other nodes due to limitation of communication ranges. The second method is distributed Kalman Filters (Olfati-Saber, 2007; Olfati-Saber, et al., 2005; Cattivelli, et al., 2008) where every neighbor node runs its own version of the Kalman Filter and shares the information with all other neighbors to reach the consensus of the system. The approaches above are distributed in processing. The number of neighbor nodes determines how expensive the algorithms are

in terms of power consumption and communication complexity. Consequently, these approaches are not efficient because they require extensive inter-communication among neighbor nodes. In comparison with the distributed version of Kalman Filter in literature (Rao, et al., 1991; Olfati-Saber, 2007; Alriksson, et al., 2007; Olfati-Saber, et al., 2005; Cattivelli, et al., 2008; Hashemipour, et al., 1998), our version of the distributed Kalman Filter simplifies computational burden and reduces inter-node communication. Thus, the total power consumption in the entire sensor network is lower than that reported elsewhere in the literature.

Our approach is different from the above work in the sense that the Kalman Filter is implemented in a distributed fashion across the WSNs. At a given instant, only one master node runs the Kalman Filter using the measurement inputs from its neighbors and shares the estimated knowledge with the subsequent master node. The neighbors within a certain distance from the target measure the distance to the target, and transmit measurements to the master node. On one hand, the procedure significantly reduces the communication costs among the neighbor nodes in comparison with the algorithms proposed in (Rao, et al., 1991; Olfati-Saber, 2007; Alriksson, et al., 2007; Olfati-Saber, et al., 2005; Cattivelli, et al., 2008; Hashemipour, et al., 1998). On the other hand, since the master node alone executes the Kalman Filter and the neighbor nodes only perform measurement functions, the complexity of the WSN is greatly reduced.

Another contribution of this paper is that the master node determines the direction and velocity of the intruder and wakes up appropriate sensor nodes in the direction of the target travel. As the target moves into the sensing range of a sensor node, it is already activated and is ready to take measurements. Whereas the other nodes that are far away from the target are automatically turned off to save energy. The master node also decides to wake up sufficient nodes to take measurements. By knowing the maximum target's velocity, the boundary nodes of the sensor field are activated in round robin fashion discussed in (Watfa, et al., 2006b) to save energy.

Unlike other approaches mentioned above, we do not make an assumption about the linear movement of the target. In this paper, the distributed Kalman Filter is proposed to estimate the position of the target. This approach is validated through simulation examples and the results are compared with those represented in literature. We show the main contribution, the approach, validations, and comparison between our method and the previous

work on distributed Kalman filtering. The algorithm was also able to track the target with random directions with acceptable estimated results. The estimation results showed that the model is robust to measurement noise and the change in velocity. The estimated knowledge of the Kalman Filter including system state and covariance matrix is passed directly to the subsequent master node where the Kalman Filter is run. Consequently, the performance of the distributed Kalman Filter is as good as that of the centralized Kalman Filter.

The rest of the paper is organized as follows: Section 2 discusses the algorithm in details. In section 3, we show the numerical simulation. Section 4 and 5 are discussion and conclusion.

## 2 ALGORITHM

### 2.1 Problems and Assumptions

A sensor field is densely deployed with sensor nodes. It is assumed that each node has omnidirectional sensing capability to measure the distance between the target and itself. Moreover, every node knows its coordinates in the sensor field, and all nodes are stationary. Initially, all the nodes except those at the boundary of the monitored area are assumed to be in sleep mode. Assuming that there is an intruder entering the sensor field with an unknown nonlinear trajectory and a known maximum velocity, the problem is to track the position of the intruder accurately. When a target moves in the sensor field, the nodes close to the target will automatically activate and sense the target.

All sensing nodes are within one communication hop from the master node. The trilateration algorithm requires that every point in the field is covered by at least three sensor nodes.

A node can be either the master node or a measurement node. Nodes take measurements and sends data to the master node if they are actively in the sensing region. Concurrently, the master node collects data from its neighbors, running estimation algorithms and broadcasting the information of the target to its neighbors, including the target's current coordinates and direction. Depending on the information from the master node, the neighbor nodes around the target automatically turn off when they are not in the region of activation  $R$  around which is defined as the following.

The target, represented by  $\star$  symbol shown in Figure 1, is moving in horizontal direction. The

region  $R$  is defined by the circle radius  $R_1$ , the radius of  $R_2$  and angle  $2\alpha$  – the region limited by the bold line.  $R_2$ ,  $R_1$ , and  $R_a$  ( $R_2 > R_1 > R_a$ ) are activation radius, sensing radius, and measurement radius respectively. All the sensor nodes inside the region of activation  $R$  are activated, while the nodes outside the region are in sleep mode to save power. All the nodes inside the circle  $(O, R_1)$  can sense the target while no node outside can detect the target. However, only nodes inside the circle  $(O, R_a)$  are actively taking measurements and reporting the data to the master node. This is done to account the imprecision in the location information of a given sensor node. For example, if there is 20% uncertainty in measurement accuracy then the solution  $R_1=1.2R_a$  can ensure that there are no sensor nodes outside the circle  $(O, R_1)$  that can detect the target  $\star$ . Assuming that the maximum target velocity is known, and the direction of the target does not change sharply. The selection of  $R_2=1.8R_a$  and  $2\alpha = 60^\circ$  can guarantee the sensors in the moving direction of the target are activated in advance. Thus, the WSN can track the target continuously without any interruption.

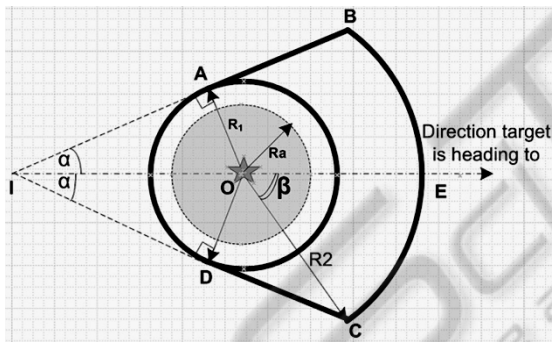


Figure 1: The target represented by  $\star$  at point  $O$ . The boundary of the region of activation  $R$  is limited by line  $AB$ , curve  $BC$ , line  $CD$  and curve  $CA$  (the bold line above). The curve  $BC$  is formed by part of the circle  $(O, R_2)$ . No nodes outside circle  $(O, R_1)$  can sense the target. All the nodes inside  $R$  are activated. However, only the sensors inside the circle  $(O, R_a)$  are actively taking measurement.

## 2.2 Settings

Initially, the sensor nodes in the boundary of the field are on to detect intruders while the all other sensors are off. If the maximum velocity of a target is known, then the boundary nodes can turn on and off periodically without losing the ability to track the incoming target according to (Wafra, et al., 2006b). When the boundary nodes detect an intruder, the

region  $R$  is formed and the nodes inside are activated.

A master node is selected depending on two criteria: the distance to the target and power residual. The sensors inside the circle with radius  $R_a$  take measurements and transfer the measured data to the master node. The master node runs the Kalman Filter and obtains the estimated position and the direction of the target. The master node broadcasts the learned knowledge of the target to its neighbors. After receiving the information, a node will turn on or off depending on whether it is inside or outside region  $R$ .

## 2.3 Position Calculation

After receiving the measurement from the target's neighbor sensor nodes, the master node uses the trilateration and the least square algorithm to calculate the position of the target.

Suppose there are  $k$  sensor nodes that are actively taking measurements whose coordinates are  $(x_1, y_1); (x_2, y_2); \dots (x_k, y_k)$ , and measured distances from each nodes to the target are  $d_1, d_2, \dots, d_k$  respectively.

The least square solution of the target's coordinate  $(x_t, y_t)$  is:

$$\begin{bmatrix} x_t \\ y_t \end{bmatrix} = (A^T A)^{-1} A b \quad (1)$$

where  $A$  and  $b$  are in the following form:

$$A = \begin{bmatrix} 2(x_2 - x_1) & 2(y_2 - y_1) \\ 2(x_3 - x_2) & 2(y_3 - y_2) \\ \dots & \dots \\ 2(x_k - x_{k-1}) & 2(y_k - y_{k-1}) \\ 2(x_1 - x_k) & 2(y_1 - y_k) \end{bmatrix} \quad (2)$$

$$b = \begin{bmatrix} (d_1^2 - d_2^2) + (x_2^2 + y_2^2) - (x_1^2 + y_1^2) \\ (d_2^2 - d_3^2) + (x_3^2 + y_3^2) - (x_2^2 + y_2^2) \\ \dots \\ (d_{k-1}^2 - d_k^2) + (x_k^2 + y_k^2) - (x_{k-1}^2 + y_{k-1}^2) \\ (d_k^2 - d_1^2) + (x_1^2 + y_1^2) - (x_k^2 + y_k^2) \end{bmatrix} \quad (3)$$

## 2.4 Power Consumption

The transmitted power  $P_{Tx}$ , received power  $P_{Rx}$ , idle power  $P_i$  and sleeping power  $P_s$  are 1400 mW, 1000 mW, 830 mW, and 130 mW respectively based on the power consumption analysis in (Wafra, et al.,

2006b). From region  $\mathbf{R}$ , the number of sensor nodes inside the circle radius  $R_a$  is  $N_a$ .  $N_i$  is the number of sensor nodes outside the circle with radius of  $R_a$ , but inside the region  $\mathbf{R}$ . The number of sensor nodes in the sensor field and number of active sensor nodes in the boundary are  $N$  and  $N_b$  respectively. The total power consumption of the sensor field in one sampling cycle is calculated as following.

The  $N_a$  neighbors make  $N_a$  transmissions and the master node receives  $N_a$  times.

$$P_{meas} = N_a(P_{Tx} + P_{Rx}) \quad (4)$$

The master node broadcasts the target position and its directions, and it makes one transmission. Each of  $(N_a + N_i)$  neighbors in the cone area receives the information of the target once.

$$P_{broadcast} = (N_a + N_i)P_{Rx} + P_{Tx} \quad (5)$$

Each active node, except measurement nodes, consumes an amount of the idle energy

$$P_{idle} = (N_b + N_i)P_i \quad (6)$$

The other nodes are sleeping, and the total power consumed by these nodes is

$$P_{sleep} = (N - N_a - N_i - N_b)P_s \quad (7)$$

Then total consumed power is

$$P_w = P_{meas} + P_{broadcast} + P_{idle} + P_{sleep} \quad (8)$$

## 2.5 Distributed Kalman Filter

Local prediction (see (Rao, et al., 1991))

$$\begin{aligned} \hat{x}(k+1|k) &= F(k) \times \hat{x}(k|k) \\ P(k+1|k) &= F(k) \times P(k|k) \times F^T(k) + Q \end{aligned} \quad (9)$$

Local update

$$\begin{aligned} P^{-1}(k+1|k) &= P^{-1}(k|k) + H^T(k+1) \times R^{-1}(k+1) \times H(k+1) \\ W(k+1) &= P(k+1) \times H^T(k+1) \times R^{-1}(k+1) \\ \bar{x}(k+1|k+1) &= \hat{x}(k+1|k) + W(k+1) \\ &\quad \times [z(k+1) - H(k+1) \times \hat{x}(k+1|k)] \end{aligned} \quad (10)$$

Where  $z(k+1)$  is the target position calculated in (1). The knowledge passed to the subsequent master node  $\bar{x}(k+1|k+1)$  and  $P(k+1|k+1)$

## 3 NUMERICAL EXAMPLES

We will consider two scenarios to demonstrate the distributed Kalman Filter for target tracking. In the first, it is assumed that sensor nodes are uniformly distributed. This requirement is relaxed in the second scenario where the nodes are randomly deployed. It is assumed that there is no hole in coverage within the regions to be monitored, and every point is covered by at least three sensors.

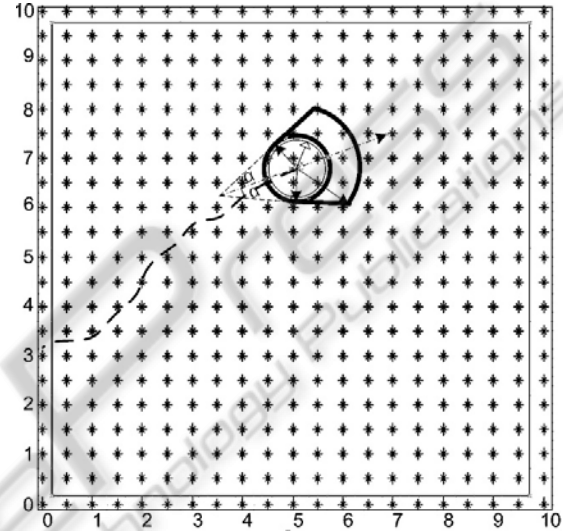


Figure 2: Example of sensor field and the trajectory of the target. The sensor nodes in the boundary of the field are always active. In the figure, all the nodes in the cone area around the target are activated.

The sensor field is assumed to be a square of the dimension  $10 \times 10$  units as seen in Figure 2. By choosing the distance of any two closest nodes is 0.5 units, the total number of uniformly distributed sensor nodes is 441. The target is assumed to move along the horizontal trajectory with the sinusoid velocity profile while the vertical coordinate remains at  $y = 5$ . In 10 seconds, the target travels between the coordinates  $(0, 5)$  and  $(10, 5)$ . The sampling frequency is 200Hz and the simulation time is 10 seconds. The following difference equations are used to model the dynamic behaviors of the moving target.

$$\begin{aligned} x_{k+1} &= Fx_k + w_k \\ z_k &= Hx_k + v_k \end{aligned} \quad (11)$$

$$\text{Where } F = \begin{bmatrix} 1 & 0 \\ \Delta t & 1 \end{bmatrix}, x_k = \begin{bmatrix} v_k \\ p_k \end{bmatrix}, H = [0 \ 1]$$

$x_k$  is the target velocity and  $p_k$  is target position in x the direction at time  $k$ .  $\Delta t$  is the sampling time.

Moreover,  $w_k$  and  $v_k$  are Gaussian distributed with zero mean state noise and measurement noise. From scenario 1 to scenario 4, the initial condition for the Kalman Filter is the same as the true value while it is nonzero in scenario 5. The sensor nodes are uniformly deployed in scenario 1 to scenario 5 while randomly deployed in scenario 6.

**Scenario 1:** Without using the Kalman Filter, more sensors used in measurement results in better estimated tracking. As seen in Table 1, when the average measured sensor nodes increased from 4.5 to 17.5, the noise variance decreased from  $21.71 \times 10^{-3}$  to  $13.49 \times 10^{-3}$ . However, the trade off is the total power consumption of the network increases from  $1.38 \times 10^5$  to  $2.09 \times 10^5$  (mW). The power consumption analysis is shown in Figure 3.

Table 1: Performance analysis.

Average measured sensors	Average active sensors	Error variance without Kalman Filter ( $\times 10^{-3}$ )	Error variance with Kalman Filter ( $\times 10^{-3}$ )	Average total power consumption (mW $\times 10^5$ )
4.5	9.3	24.71	3.63	1.38
17.5	39.2	13.49	1.57	2.09
60.4	139.9	7.03	0.98	4.48
130.8	275.5	4.62	0.31	7.88
279.1	416.2	5.43	0.10	12.60

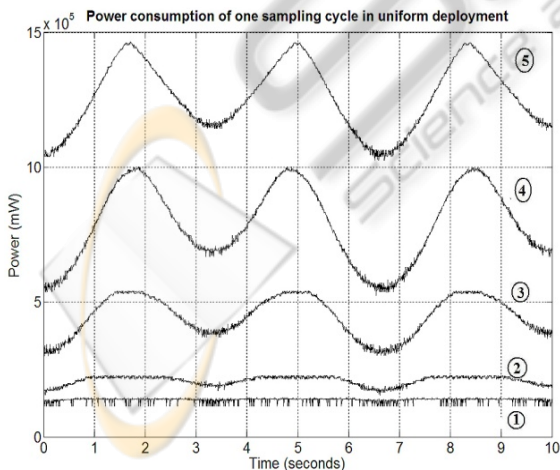


Figure 3: Without the Kalman Filter, the line number 1, 2, 3, 4, and 5 have average measured sensor nodes of 4.5, 17.5, 60.4, 130.8, and 279 respectively. For the line number 3 to 5, the total power consumption is fluctuated because when the target moves close to the boundary the

number of active sensors is reduced. Then the total power consumption reduces. Line #1 and #2 are quite flat because in these scenarios the relatively small cone regions result in small difference in the number of active sensors when the target in the middle of the field and when it is close to the boundary.

**Scenario 2:** When the Kalman Filter is used, the variance of the estimated error is smaller and Figure 4 shows the smoother tracking performance compared to scenario 1. As shown in Table 1, by using the Kalman Filter, only an average of 4.5 measured sensors is sufficient to achieve the error variance of  $3.63 \times 10^{-3}$  which is smaller than  $5.43 \times 10^{-3}$  resulted by an average of 279.1 measured sensors without using Kalman filtering.

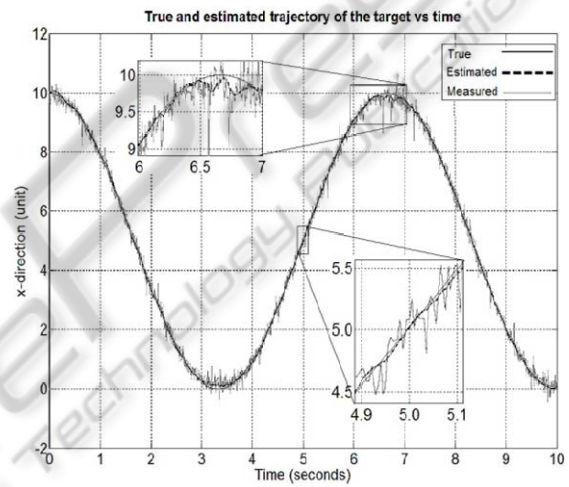


Figure 4: Target's true trajectory is the solid black line, and its estimations using trilateration with the Kalman Filter and without the Kalman Filter are the solid gray line and the dashed black line respectively. The average number of measured sensors is 4.5, and the standard deviation of state noise and measurement noise are 0.01 and 0.2 respectively. The Kalman Filter yielded both a smaller error variance and smoother estimated trajectory. As we zoom in two small sub figures, the estimated position is close to the true position when the target moves in a linear part of the sinusoid trajectory. Without using the Kalman Filter, the estimated trajectory is noisy.

**Scenario 3:** When the number of average measured sensors and the sampling frequency are fixed, slower average velocity results in smaller estimated tracking error as shown in Figure 5. In this scenario, the sampling frequency is 200Hz, the standard deviation of state noise and measurement noise are 0.01 and 0.2 respectively, and the average number of measured sensors is 6.3.

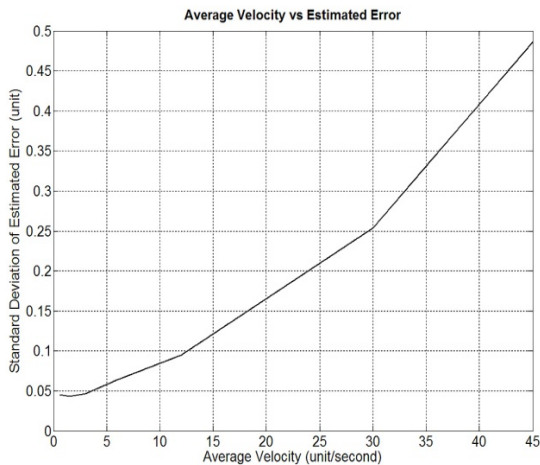


Figure 5: Average velocity increases as the estimated error has a larger standard deviation.

**Scenario 4:** In this scenario, the sampling frequency is kept at 200Hz, average target velocity is three units per second and the average number of measured sensors is 6.5. In Figure 6, the standard deviation of state noise is fixed at 0.01 while the measurement noise has a standard deviation varying from 0.01 to 0.5. The variance of estimated error increases with the increase in measurement noise. In addition, with the same number of average measured sensors of 6.5, the smaller measurement noise leads to the better tracking performance. The tracking performance, shown in Figure 7, is better when the measurement noise is smaller.

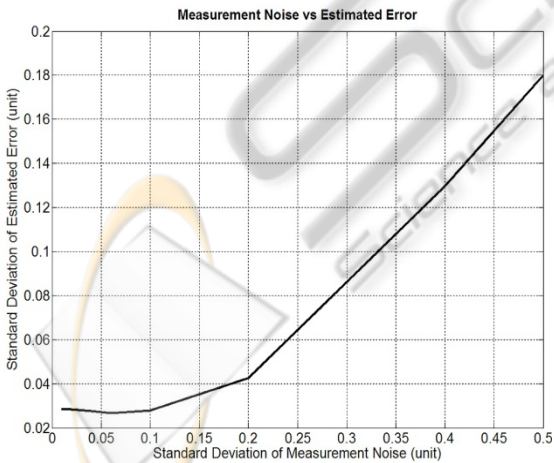


Figure 6: When the distance measurement is subjected to a larger noise, the variance of estimated tracking error becomes bigger.

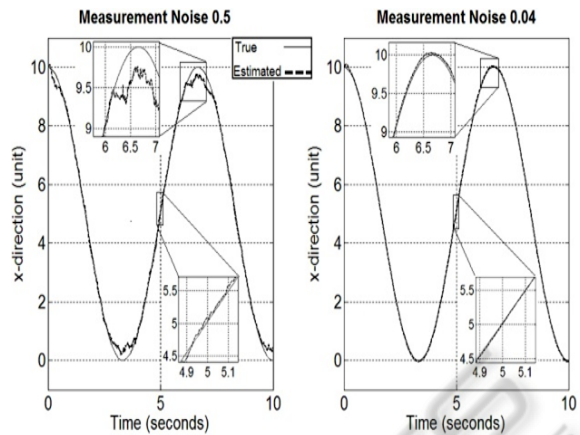


Figure 7: The true and the estimated trajectory with different measurement noise levels. The standard deviation of measurement noise is 0.5 in the left side while it is 0.04 on the right side.

**Scenario 5:** When the master node does not share the knowledge of the target including the target state and the covariance matrix with the subsequent one, the subsequent master node has to run the Kalman Filter with the default initial conditions. Assuming that the difference between the initial position and the actual target position is the measurement error, the change in master nodes is indicated by the abrupt jumps in estimated error as shown in Figure 8. When there is a change in the master node, the Kalman Filter requires some extra time steps to converge.

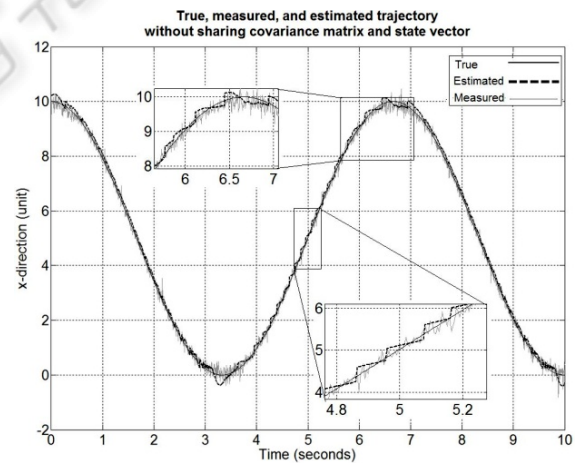


Figure 8: Without sharing the state vector and covariance matrix to the subsequently master node, each master node has to start the Kalman Filter from scratch. The measurement noise standard deviation is 0.2, while the number of average measured sensor nodes is 7.6.

**Scenario 6:** As shown in Figure 9, when the sensor nodes are randomly distributed, we get similar results in comparison with the uniform scenario

shown in Figure 3. However, the power consumption is not as smooth as it is in the uniform scenario. Due to the random nature, there are more sensor nodes covering a specific point while fewer sensor nodes are covering other points. In order for our algorithm to work effectively, at least three sensor nodes must cover each point in the sensor field

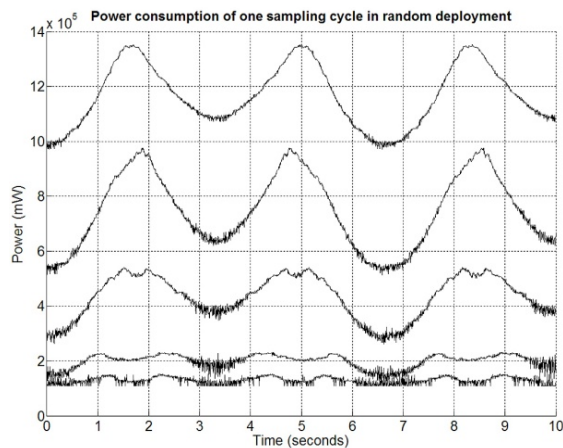


Figure 9: Power consumption of one sampling cycle in random deployment. There are 441 sensor nodes deployed in the sensor field of  $10 \times 10$ . The line number 1, 2, 3, 4 and 5 have average measured sensors of 3.4, 15.7, 59.5, 127.2, and 259.7 respectively.

## 4 DISCUSSIONS

The above results show that the distributed Kalman Filter implementation in a WSN is successful in tracking moving targets. The tracking error is small when the target follows a linear trajectory while nonlinear trajectories with high target velocities result in higher tracking errors. However, in all these scenarios, the tracking error is 12.5% smaller than that obtained in the absence of the Kalman Filter. In addition to the improved tracking performance, the distributed filter requires fewer nodes to be active at any given instant, thereby reducing the overall power consumption of the WSN. This is significant because the lowered power consumption increases the useful life of the WSN.

The choice of the cluster head is determined by the residual power ( $P_{residual}$ ) of each node and its distance to the target. At each instant, every active node in the proximity of the target computes the weighted sum of its residual power and its distance to the target ( $D$ ) as following  $W_{node} = \alpha D + \beta P_{residual}$  with constants  $\alpha$  and  $\beta$  in the interval

[0, 1]. A node will become the new master node if its weighted sum is smaller than that of the current master node. Consequently, the knowledge of the Kalman filtering is transferred from the current master node to the new one.

## 5 CONCLUSIONS

In this paper, a method for the target tracking problem using distributed Kalman Filter in WSNs is demonstrated. The algorithm is robust to changes in the velocity of the target and measurement noises. The algorithm reduces the total power consumption in the network in comparison with distributed Kalman Filter algorithms elsewhere in literature. Another contribution of the proposed algorithm is the activation of a reduced set of sensor nodes for target tracking. Thus, sensor nodes further away from the target are inactive and thereby conserve power. Fewer active nodes also mean reduced communication among nodes. These two factors together increase the useful life of the WSN while provide accurate tracking in the presence of measurement noise and target uncertainty.

The results presented in this paper assume that each sensor node knows its position accurately and share a common system clock with other nodes. This is not a detriment as results in time synchronization and localization already exist in the literature. Proof of the convergence of the tracking error and the stability of the overall system will be presented in an extended version of the paper.

## REFERENCES

- Akyildiz, I. F., Su, W., Sankarasubramaniam, Y., & Cayirci, E. (2002). A survey on sensor network, *IEEE Communications Magazine* (Vol. 40 pp. 102-114).
- Al-Karaki, J. N., & Kamal, A. E. (2004). Routing techniques in wireless sensor networks: a survey. *Wireless Communications, IEEE, 11(6)*, 6-28.
- Alriksson, P., & Rantzer, A. (2007, December 12-14 ). *Experimental Evaluation of a Distributed Kalman Filter Algorithm*. Paper presented at the 2007 46th IEEE Conference on Decision and Control, New Orleans, LA
- Cardei, M., Thai, M. T., Li, Y., & Wu, W. (2005, March 13-17). *Energy-efficient target coverage in wireless sensor networks*. Paper presented at the INFOCOM 2005. 24th Annual Joint Conference of the IEEE Computer and Communications Societies, Miami, Florida.

- Cattivelli, F. S., Lopes, C. G., & Sayed, A. H. (2008, June). *Diffusion strategies for distributed kalman filtering: Formulation and performance analysis*. Paper presented at the Proc. 2008 IAPR Workshop on Cognitive Information Processing, Santorini, Greece.
- Chen, M., Gonzalez, S., & Leung, V. C. M. (2007). Applications and design issues for mobile agents in wireless sensor networks. *IEEE Wireless Communications*, 14(6), 20-26.
- Chiang, C., Wu, H., Liu, W., & Gerla, M. (1997, April). *Routing In Clustered Multihop, Mobile Wireless Networks With Fading Channel*. Paper presented at the In Proc. IEEE SICON'97.
- Hashemipour, H. R., Roy, S., & Laub, A. J. (1998). Decentralized structures for parallel Kalman filtering. *IEEE Transaction on Automatic Control*, 33(1), 88-94.
- Inatanagonwivat, C., Govindan, R., & Estrin, D. (2000, August). *Directed Diffusion: A Scalable and Robust Communication Paradigm for Sensor Networks*. Paper presented at the In Proceedings of the Sixth Annual International Conference on Mobile Computing and Networking (MobiCOM '00).
- Kim, J.-H., West, M., Scholte, E., & Narayanan, S. (2008, June 11-13). *Multiscale consensus for decentralized estimation and its application to building systems*. Paper presented at the 2008 American Control Conference, Seattle, WA
- Mutambara, G. O. (1998). *Decentralized estimation and control for multisensor systems*: CRC Press.
- Olfati-Saber, R. (2007, December 12-14). *Distributed Kalman filtering for sensor networks*. Paper presented at the 2007 46th IEEE Conference on Decision and Control, New Orleans, LA
- Olfati-Saber, R., & Shamma, J. S. (2005, December 12-15). *Consensus Filters for Sensor Networks and Distributed Sensor Fusion*. Paper presented at the 44th IEEE Conference on Decision and Control, CDC-ECC'05.
- Rao, B. S., & Durrant-Whyte, H. F. (1991). Fully decentralized algorithm for multisensor Kalman filtering. *IEE Proceedings-D Control Theory & Application*, 138(5), 413 - 420.
- Uhlmann, J. K. (1996). General data fusion for estimates with unknown cross covariances. *Proceedings of SPIE*, 2755, 536-547.
- Wafra, M. K., & Commuri, S. (2006a, August 14). *The 3-Dimensional Wireless Sensor Network Coverage Problem*. Paper presented at the 2006 IEEE International Conference on Networking, Sensing and Control. ICNSC '06, Ft. Lauderdale, FL.
- Wafra, M. K., & Commuri, S. (2006b). *Optimal sensor placement for Border Perambulation*. Paper presented at the 2006 IEEE International Conference on Control Applications, Munich, Germany.